RSC Advances

ROYAL SOCIETY OF CHEMISTRY

www.rsc.org/advances

Synergistic effect of microwave irradiation and conjugated polymeric catalyst in the facile degradation of dyes

Ufana Riaz* and S.M.Ashraf[+]
Materials Research Laboratory
Department of Chemistry Jamia Millia Islamia (A Central University), New Delhi-110025, India
*Corresponding author: Fax-(+91-112-684-0229); *E-mail address*- (ufana2002@yahoo.co.in)
[+] Now retired

Abstract

Microwave-enhanced photodegradation of dyes is one of the emerging and promising technologies for waste water remediation. Microwave effectively accelerates photocatalytic degradation, but only in presence of a suitable photocatalyst such as TiO_2,ZnO and also when microwave electrodeless lamp (MEL) substitutes traditional lamp as light source. As the existing inorganic photocatalysts have been proven to be potentially toxic to the aquatic environment, this remediation technique can be extremely simplified if the photocatalyst can be replaced by a benign catalyst which can work under microwave irradiation in the absence of any external light source. In the present study, attempt is made for the first time to degrade and mineralize Orange G (OG) dye in a laboratory microwave oven at 30°C, using an organic catalyst, poly(1-naphthylamine) (PNA), a conjugated polymer synthesized by enzymatic method. PNA was characterized by relevant experimental techniques. The degradation was carried out by exposing the OG dye solutions to microwave irradiation for different time intervals in absence of UV-vis radiation and TiO_2. PNA as a catalyst was found to enhance the dye degradation under microwave irradiation by almost two times as compared to its degradation under microwave alone. 100 ppm of OG dye solution was found to degrade upto 90% in 20 min at 30°C in presence of PNA. The same solution revealed mineralization upto 85% in 40 min as confirmed by the total organic content (TOC) analysis. With the help of LC-MS, seven intermediates were identified ranging between m/z 227 to m/z 97, on the basis of which a tentative degradation pathway of the dye has been proposed. Dye degradation in presence of PNA as a microwave catalyst under present experimental setup was found to yield results better than other photocatalytic or microwave-assisted photocatalytic degradation methods.

Introduction

Approximately 1–20% of the total synthetic dyes in the world are released as textile effluents[1-2]. Azo dyes belong to the largest class of dyes used in textile and paper industries. They are stable to ultraviolet and visible light irradiation, resistant to aerobic degradation and can be reduced to potentially carcinogenic aromatic amines under anaerobic conditions[3-5]. Hence, methods by which the degradation and mineralization of such dye effluents can be achieved have received considerable attention. Of late, efforts have been made to completely degrade and mineralize dyes for remediation of industrial waste water using advanced oxidation process (AOP)[6], photocatalysis[7] and sonophotocatalysis[8] etc.

Much attention has been focused on photocatalytic degradation of organic pollutants mediated by nano TiO_2 in the past two decades. Lately, the International Agency for Research on Cancer (IARC) has classified TiO_2 as "*possibly carcinogenic for humans*"[9]. The various possible sources of contamination of water bodies by nano-TiO_2 warrant assessing its effects on ecosystems, and public health. There are a paucity of studies about the presence of nano-TiO_2 in the environment. TiO_2 nano particles have been detected in river waters, while TiO_2 concentrations of about 16 µg/L were found in urban runoff [10-11]. The potentially harmful effects of TiO_2 necessitate the need for development of green catalysts and investigation of their toxicity to ensure sustainable use.

Conducting polymers such as polyaniline (PANI) and polpyrrole (Ppy) with extended π-conjugated electron system and good environmental stability have been widely used as stable photosensitizers for enhancing the photocatalytic activity of TiO_2 [12-13]. However, none of the above mentioned conjugated polymers have been reported to be used alone as a catalyst for wastewater remediation. Microwave coupled photocatalytic degradation of dyes and organic pollutants using TiO_2 based catalysts has been found to enhance the degradation of the organic pollutants through the generation of electrons and holes which further produce $H^{\bullet}$, $OH^{\bullet}$, and $O_2^{\bullet-}$ free radicals.The nonthermal effects like hot spots, production of surface defects in TiO_2, formation of additional charge carriers and additional trap sites also enhance the dye degradation[14-18]. So far no thorough investigation pertaining to the degradation of dyes under microwave irradiation alone, entirely in absence of UV or visible light, has been undertaken, nor a catalyst other than inorganic semiconductors have been used for the above end.

We have earlier reported the role of poly(1-naphthylamine) (PNA) - a PANI derivative as a latent photocatalyst in the sonophotocatalytic degradation of Commassie blue dye[19]. PNA was found to be a good adsorbent of the dyes[20] and possesses surface properties that facilitate the mineralization of the dyes through the adsorption of the intermediates. With the aim to prepare a benign catalyst that can provide catalytic efficiency similar to an inorganic semiconductor photocatalyst in absence of any UV-visible light, we report, for the first time, the enzymatic synthesis of poly(1-naphthylamine) (PNA) and its catalytic effect under microwave irradiation alone on the degradation of Orange G (OG) dye. An advance laboratory microwave oven with controls for temperature, time and rate of heating was used as microwave irradiation source. The degradation of the dye was monitored spectrophotometrically and mineralization was studied by TOC analysis at different times. Degradation intermediates of the dye formed at 20 minutes of irradiation were analyzed by liquid chromatography-mass spectroscopy (LC-MS). The generation of $OH^{\bullet}$ free radicals and its role in the degradation of dye was investigated using isopropanol (i-PrOH) as scavenger. It was observed that though microwave radiation alone was able to degrade OG dye in the present experimental set up, PNA was found to remarkably enhance its degradation rate. The toxicity of the reaction intermediates, were also carried out to provide an insight about their influence on the environment. On the basis of LC-MS results, a tentative degradation pathway of Orange G dye in presence of PNA was proposed.

Experimental

Materials

1-naphthylamine (Sigma Aldrich, USA) was distilled under reduced pressure over a mixture of stannous chloride and potassium hydroxide prior to use. Hydrogen peroxide (H2O2) (30 wt% solution), ammonium persulfate, D-10 camphor-10-sulfonic acid (CSA), horseradish peroxidase(HRP, Type II, 240 U/mg, RZZ1.9), Orange G dye, isopropanol, and benzoquinone were acquired from Sigma Aldrich, USA. All reagents were used without further purification.

Enzymatic synthesis of poly (1-naphthylamine)

0.002 M of 1-naphthylamine and 0.002 M of doping acid (CSA) were added in a three neck 50 mL reactor and kept under vigorous magnetic stirring in an ice bath maintained at -10°C. 0.2 mL of freshly prepared HRP solution stock solution (10 mg/ml in pH 6.0, 0.1 M phosphate buffer) was then added to the reaction media. The reaction was initiated by adding 22.7 mL of 0.3 wt% H_2O_2 solution (added in 4 portions of 5.7 mL each) at the interval of 3 min. This procedure avoids inactivation of the enzyme by excess of hydrogen peroxide in the reaction media. After 2.5 h of reaction time, the obtained purple PNA dispersion was collected by centrifugation. PNA was washed several times with deionized water and methyl alcohol. It was then dried in vacuum oven at 80°C overnight. The yield of the polymer was 78%.

Degradation studies

OG dye of concentrations 50 mg/L 100 mg/L and 200 mg/L were prepared by dilution of a stock solution of 500 mg/L and were labeled as OG-50, OG-100, and OG-200 respectively. The solutions (100 ml each) were irradiated with microwave in Ladd Research Microwave oven model LBP-250, USA, (Fig.1), fitted with a time and temperature controller. The rate of heating upto the desired temperature (30°C) was done by an in-built 'ramp controller'. The temperature was measured by a temperature probe located at the centre of the beaker. The solutions were stirred by bubbling O_2 through them. The solutions were exposed to microwave irradiation in a batch process for 4, 8, 12, 16, 20, 30, and 40 minutes. 10 mL dye solution at each irradiation time of each set was taken out and analysed spectrophotometrically. All the experiments were repeated by adding 150 mg of poly (1-naphthylamine) (PNA) in each of OG-50, OG-100 and OG-200 dye solutions.The solutions were marked serially as PNA-OG-50, PNA-OG-100, PNA-OG-200 and were shaken for one hour in the dark for establishing equilibrium. The solutions were then irradiated at 30°C in the above microwave oven under continuous bubbling of O_2. 10 mL supernatant of the PNA-OG dye solution was taken and centrifuged for 10 min at a speed of 5000 rpm and analyzed as earlier. The duplicate set was run for each concentration. The concentration of the dye was found out by measuring the absorbance on a Shimadzu-UV1800, Japan, spectrophotometer.

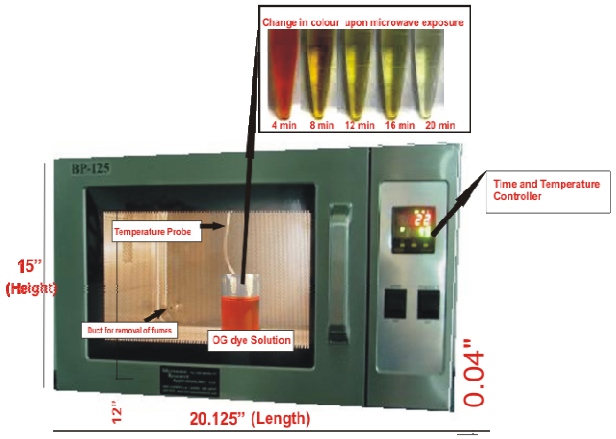

Fig. 1 Laboratory microwave oven used for degradation studies

Characterization

Spectral Analysis

FT-IR spectra were obtained using KBr pellets on a Shimadzu IR Affinity FT-IR spectrophotometer The UV–vis spectra of the PNA dispersions were obtained on a Shimadzu UV-1800 spectrophotometer. The spectra were taken in NMP. To obtain the spectrum of the undoped form, PNA particles were dedoped by treatment with ammonia solution.

Molecular weight, surface area and zeta potential measurements

GPC measurements were carried out on 148 a Viscotek GPC Max AUTO sampler system consisting of a 149 pump, a Viscotek UV detector, and a Viscotek differential 150 refractive index (RI) detector. A ViscoGEL GPC column 151 (G2000HHR) (7.8 mm internal diameter, 300 mm length) was used. The effective molecular weight range of the column used was 456−42,800. THF was used as an eluent at a flow rate of 1.0 mL/min at 30°C. Both detectors were calibrated with 155 polystyrene (PS) standard having narrow molecular weight distribution.

Surface area was determined by Brunauer Emmett and Teller (BET) method using Micromeritics ASAP 2100 with N2 adsorption at temperature of 77.40 K.

Zeta potential was determined by using a ZEN 3600 Model Zetasizer Nano-ZS connected with MPT-2 multipurpose automatic titrator (Malvern Inst. Ltd., UK). The optical device contains a 5 mW He–Ne (638 nm) laser. A sample of 0.1 g suspension of PNA was sonicated for 10 min. The suspension was then kept still for 5 min to let larger particles settle. About 10 ml of clear supernatant was placed into the vial, which was connected with the automatic titrator to measure the Zeta potential.

Mineralization measurements

Mineralization of the dye was determined by measuring the total organic content (TOC) of the degraded dye at 4, 8, 20, 30 and, 40 minutes on Shimadzu TOC-5000A total organic carbon analyzer.

LC-MS Analysis

Liquid chromatography-mass spectroscopy (LC-MS) was conducted using a Finnigan LCQ ion trap mass spectrometer equipped with an electro spray ionization interface (ESI) source and operated in negative polarity mode fitted with a Genesis, C-18 column (4.6 × 250 mm) containing 4 µm packed particles (Alltech, Deerfield, Germany). Acetonitrile and 0.03 M ammonium carbonate buffer, pH 7.7, were used as eluents. The pump program was set as follows: isocratic 20% acetonitrile: 80% buffer held for 2 min; grading to 100% acetonitrile over 10 min and held at 100% for 7 min. The diode array detector allowed for concomitant recording of spectra from 200 to 600 nm. The gradient HPLC separation was coupled with LC/MSD trap 6310, ion trap mass spectrometer (Agilent technologies).

Toxicity measurements

Acute toxicity determinations were carried out by measuring the respiration inhibition in *Escherichia coli* cultures, by using FIA-conductometric methodology which was composed of a peristaltic pump, the samples and standards injector, a diffusion cell, a conductivity cell, reagent delivery tubes, ion exchange resins, a conductivity meter, a recorder, and a water bath[21]. The sterilized culture media for *E.coli* was composed of K_2HPO_4 (7.0 g), KH_2PO_4 (3.0 g), sodium citrate (0.5 g), ammonium sulphate (1.0 g), magnesium sulphate (0.2 g) and glucose (20 g) (final volume: 1 L with deionized water; pH: 7.2).The culture medium was inoculated with the bacteria and left in an oven at 37°C until the bacterial suspension became cloudy. It was then placed in a water bath at 37°C, and the CO_2 was monitored until its concentration reached 0.50 mmol L^{-1}.100 mL aliquots was transferred from this bacteria stock suspension to 250 mL Erlenmeyer flasks. Another 50 mL buffer was added into this and was kept as control solution. 100 mL bacterial suupensions were transferred into sterilised 250 mL Erlenmeyer flasks containing the 50 mL of the 20 and,40 minutes minutes microwave exposed dye solutions and 150 mLof buffer solutioin containing 125 mg suspende PNA. All solutions were kept at 37°C. CO_2 evolution was monitored at 20 minutes interval upto 120 minutes standardised time in which CO_2 evolved from 0.5 mmol L^{-1} to 4.0 mmol L^{-1}. The cultures were monitored as above with the following order of analysis: control, blank,test cultures. The % inhibition of bacterial growth against control was calculated from following equation.

% inhibition = {(C-T)/C}x 100 , where C is the final minus initial CO_2 concentration in the the control culture and T is the final minus initial CO_2 concentration in the test cultures[21].

Detection of $OH^{\bullet}$ radical formation

For confirming the formation of $OH^{\bullet}$ radicals, isopropyl alcohol (PrOH) was added to the dye solution at the rate of 5 mmol/L and 0.1 mmol/L and decolourization was monitored as in the earlier experiments. Benzoquinone (BQ) was used in a similar manner to confirm the formation of $O_2^{\bullet-}$ free radicals. Formation of H_2O_2 was confirmed spectrophotometrically[22].

Results and Discussion

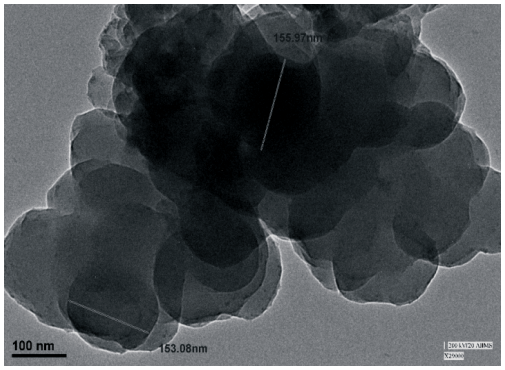

Fig. 2 TEM of PNA

Properties of the synthesized PNA

Enzymatic reactions are carried out at higher pH values than those employed in chemical synthesis to preserve peroxidase activity. When the enzymatic polymerization of 1-naphthylamine was carried out at pH 4.0, a color change to dark purple was observed indicative of polymerization of 1-naphthylamine[23]. Reactions carried out at pH of 5.0, also developed a rapid color change, but in this case to black. After the addition of H_2O_2, a

decrease of the pH was observed due to the release of CSA which is present as the 1-naphthylamine counter ion[24-27]. The pH was kept constant above 3.0 as HRP is rapidly deactivated below pH 3.0 [26-27]. As PNA doped CSA is more hydrophobic, it enhances the solubility of PNA in organic solvents and also reduces the solvation of the colloid[25-27]. 1-naphthylamine/CSA salts self-assemble in solution state to produce nanostructured morphology during polymerization. In the enzymatic oxidation, the particles grow mainly by aggregation of very small primary particles that are continuously formed during the polymerization. The conductivity of doped PNA was observed to be 3.3 x 10^{-3}S/cm while that of undoped PNA was found to be 2.7 x 10^{-11} S/cm. The molar mass of the PNA sample as determined by GPC was found to be 1834 ±18. The morphology of the dried colloidal particles was studied by TEM, shown in Fig.2. The spherical shape and the narrow size distribution of the particles, with an average diameter of 150 nm -200 nm, are observed when CSA was used as doping agent. The micrograph clearly shows formation of large aggregates which are expected to cause reduction in surface area of the PNA particle. The surface area was found to be 88 m^2/g and the average particle size around 150 nm. The PNA particles showed higher zeta potential value equal to +45 mV due to their colloidal nature.

FT-IR Analysis

The FT-IR spectrum of enzymatically synthesized PANI in aqueous medium at pH 3.0, Table.1, is quite similar to that of chemically synthesized PNA[23]. The characteristic bands of PNA were observed, such as the ring stretching of the quinoid (Q) diimine and the benzenoid (B) diamine units at 1548 cm^{-1} and 1520 cm^{-1}, respectively. Other absorption peaks were C–N stretching vibration at 1386 cm^{-1} due to the Q-B units and the 1305 cm^{-1} peak due to C–N stretching in B units. The aromatic C–H in-plane bending peak was noticed at 1170 cm^{-1}, and the peak at 728 cm^{-1} was attributed to C–H out of plane bending. The foregoing two peaks represent 2 adjacent hydrogen on naphthalene ring indicating a 1,4-disubstituted naphthalene ring[23]. The above data confirm polymerization of 1-naphthylamine through 1,4 linkage (structure given in supplimentary information).

Table 1 FT-IR spectral data of PNA

Functional group	Peak position cm^{-1}	Absorption Intensity
NH (stretching vibration)	3330	0.45
NH-Q-NHR (quinonoid)	1548	0.42
NH-B-NH (benzenoid)	1520	0.20
CN (stretching vibration)	1386 1305	0.13
CH bending (in plane)	1170	0.31
Disubstituted naphthalene ring	728	0.27

UV-visible Analysis

The UV-Vis spectrum of PNA, Fig.3, shows peaks at 350 nm in the UV range, and around 550 nm and 740 nm in the visible range. The peaks in the UV range correspond to π-π^* transitions, whereas the peaks in the visible range are attributed to the polaronic transitions[23]. The 550 nm peak depends upon dopant level whereas 740 nm peak indicates polaron delocalization due to the presence of CSA as dopant[23]. When the PNA dispersion was diluted in NH_4OH solution, a black color was developed. Two absorption bands were observed at 330 and 500-nm, the former corresponds to the π-π^* transition of the benzenoid rings and the latter is due to the exciton absorption of the quinoid rings[23]. The presence of polaronic transition peak confirmed the conducting state of the polymer[28].

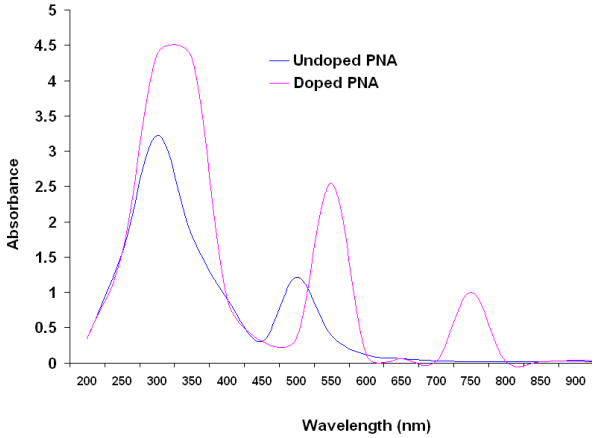

Fig. 3 UV-visible spectrum of PNA

Spectrophotmetric Analysis of dye degradation

Fig.1 shows the photographs of decolourisation of solutions of PNA-OG-100, freshly prepared, after 20 and 40 minutes of exposure of microwave radiations. OG dye shows characteristic absorption peaks at 330 nm and 480 nm[29-31]. The 480 nm peak arises from n-π* transition of azo group, while 330 nm peak results from the π-π * transition of conjugated bonds and SO_3^- groups. Other authors have also done similar assignments to these peaks[29-31]. The decrease in the absorbance intensity of the 470 nm is caused by the elimination or chemical modification of the azo group. The decrease in the absorbance intensity of the peak at 330 nm results from cleavage or modification of the benzene/ naphthalene rings, and SO_3^- groups. The points of attack of $OH^\bullet$ free radicals responsible for these modifications, are, therefore, azo linkage, naphthalene ring and sulphonate group. Plots of C/C_0 vs time of OG-50, OG-100, OG-200, PNA-OG-50, PNA-OG-100 and PNA-OG-200 solutions at different times of microwave exposure, at λ = 330 nm, and λ = 480 nm, where C_0 is the initial concentration of the dye and C is the concentration at time t are shown in Fig.4 (a) and (b). At λ= 330 nm, OG-200, OG-100 and OG-50 dye solutions show 35%, 45% and 47% degradation in 20 min. But PNA-OG-200, PNA-OG-100 and PNA-OG-50 show degradation upto 75%, 90% and 95% respectively in the same time. At λ = 480 nm, OG-200, OG-100 and OG-50 dye solutions decolorized to 48%, 52% and 55% respectively in 20 minutes. At this wavelength in the same time, PNA-OG-200, PNA-OG-100 and PNA-OG-50 decolorized to 60%, 64% and 70%-respectively. It is worth observing that the degradation of OG dye in microwave oven used at 30°C occurs without photocatalyst and UV radiation. It is observed that the decolourization of OG dye starts as the dye solutions are exposed to microwave radiations at 30°C. Since the decrease in the absorbance intensity of the two peaks occur simultaneously, it can be inferred that elimination of

benzene ring, elimination/modification of sulphonate group, elimination /oxidation of the azo linkage and oxidation/cleavage of the naphthalene group occur almost simultaneously or one after another during the decolourisation/degradation of the dye.

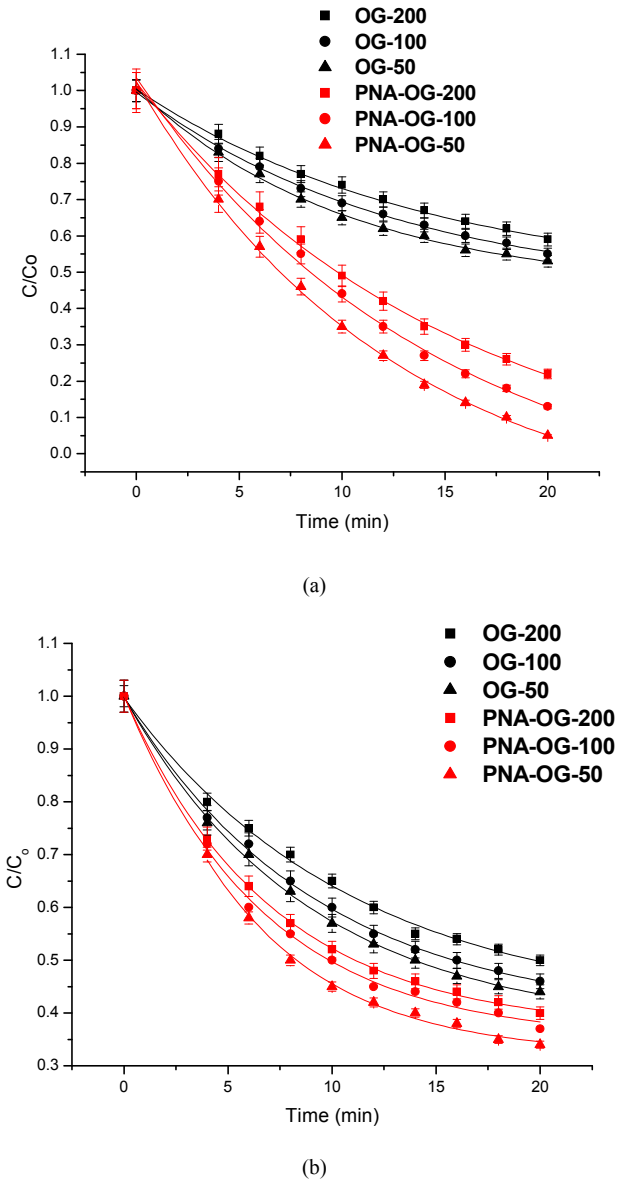

Fig. 4 Degradation of OG and PNA-OG, C/C_0 vs. time, at (a) λ=330 nm (b) λ=480 nm. Dye solution: 100 ml, PNA amount: 150 mg, Temp.: 30°C

At λ = 480 nm, there is noticeable increase in decolourisation, but much less than at λ = 330 nm, when PNA is used as catalyst. It can be inferred that although PNA provides a large surface on which $OH^{\bullet}$ free radicals and dye molecules are adsorbed; the azo groups are apparently oriented away from the surface. The $OH^{\bullet}$ free radicals sticking on the surface of PNA are, therefore, not freely available to attack the azo groups. The elimination/ chemical modification of the azo group is therefore hindered. In comparison to this, at λ= 330 nm, PNA-OG-100 shows 90% degradation while OG-100 exhibits only 45% degradation. In dye solution with PNA, the benzene and naphthalene rings, and sulphonate groups of the adsorbed dye sticks on PNA surface, and hence are accessible to attack of $OH^{\bullet}$ free radicals. In dye solution without PNA, $OH^{\bullet}$ free radicals are formed far less and are also not as effective in chemical modification of naphthalene ring, sulphonate group and azo group as on PNA surface, hence the decrease of absorption intensity is much less in this case than the dye solution with PNA. The recombination of $OH^{\bullet}$ free radicals leads to the formation of H_2O_2; the recombination increases when certain groups like azo are not cleaved or chemically acted upon easily, as life time of these free radicals is short. We have confirmed the formation of H_2O_2 spectrophotometrically which is discussed in the proceeding section.

The plot of ln C/C_0 vs time of the dye solutions OG-200, OG-100, OG-50, PNA-OG-200, PNA-OG-100, and PNA-OG 50, dye solution as such and in presence of PNA, follows the pseudo first order kinetics. Fig.5 (a) shows ln C/Co vs. time plot at λ = 480 nm. The plot shows straight lines for the dye solutions OG-200, OG-100, and OG-50. The k values for these solutions are respectively found to be 0.025 min^{-1}, 0.028 min^{-1} and 0.03 min^{-1}. Fig.5 (b) shows ln C/Co vs time plot for the peak at λ= 330 nm.

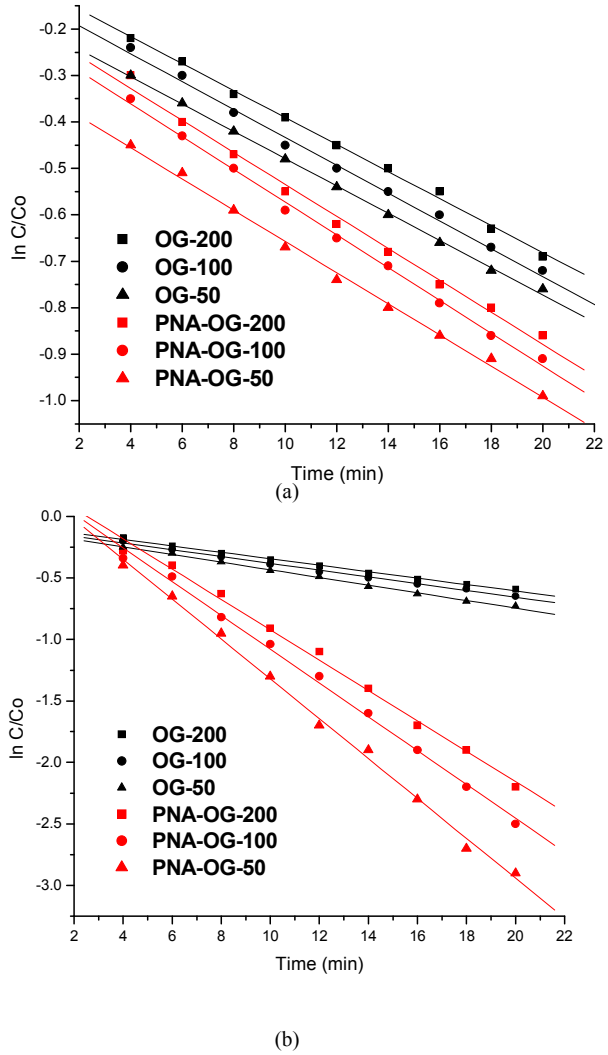

Fig. 5 Pseudo fist order rate kinetics, ln C/Co vs. time, for (a) OG and PNA-OG at λ=480 nm (b) OG and PNA-OG at λ=330 nm. .Dye solution: 100 ml, PNA amount:: 150 mg, Temp.: 30°C

The plot shows straight lines for the dye solutions OG-200, OG-100, OG-50. The straight lines indicate pseudo first order rate kinetics with k values equal to 0.026, 0.028 and 0.031 min^{-1} respectively. The dye solutions PNA-OG-200, PNA-OG-100, and PNA-OG-50, at λ = 480 nm give k values equal to 0.034 min^{-1}, 0.036 min^{-1} and 0.04 min^{-1} respectively. The k values with PNA are larger than the same without PNA. PNA thus enhances the rate of decolourisation/degradation. The k values for the dye solutions with PNA, PNA-OG-200, PNA-OG-100, and PNA-OG-50 at λ=330 nm are found to be 0.12 min^{-1}, 0.137 min^{-1} and 0.16 min^{-1} in both the cases. PNA thus increases the rate of degradation of OG dye drastically compared to the degradation of pure dye solution at similar concentrations. As dye molecules with water molecules clinging around it are adsorbed on the PNA surface; the intensity of the nonthermal effects responsible for the splitting of the water molecules into $OH^{\bullet}$ and $H^{\bullet}$ free radicals is required lesser than otherwise .This enhances the generation of these free radicals and conseqently enhances the rate of degradation and the rate constant.

The efficiency of PNA catalyst was tested by repeated degradation of OG-PNA-100 solution each time taking fresh dye solution. The used catalyst was regenerated by treating with 1N HCl overnight and then by drying it in a hot air oven at a temperature of 90-100°C. 1.0 mg of washed and dried PNA was dissolved in 10 mL of N-methyl pyrrolidone and checked spectrophotometrically (UV-vis) for any change in peak position and absorbance intensity. This also reveals intactness of chemical structure of PNA. The degradation efficiency of the catalyst was the same, i.e., 90%, till 4 cycles after which it started decreasing. Its 550 nm peak also showed 5% decrease in absorbance intensity aftr the above cycle. with same washed and dried PNA.

TOC-Analysis

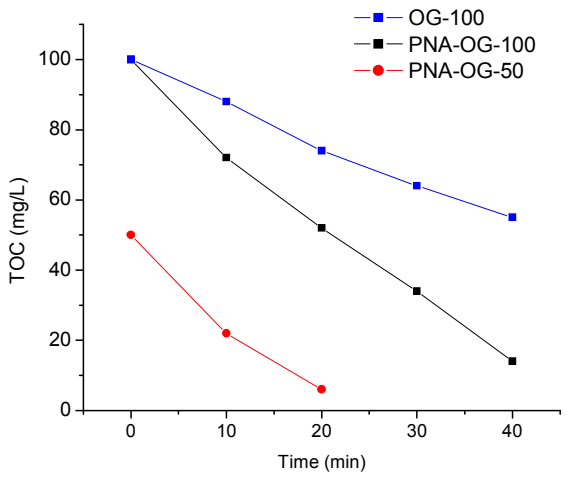

Fig. 6 TOC analysis of PNA-OG-50 and PNA-OG-100

The total organic content in mg/L gives the amount of organic material present in the analyte at different times during mineralization of the dye. OG was progressively mineralized by microwave irradiation under the conditions of the Ladd Research Microwave Oven operated at 30°C. The OG-100 dye solution is found to mineralize by 45% on exposing to microwave irradiation upto 40 min. Dye solutions, PNA-OG-100 and PNA-OG-50, show a decrease in the TOC value with time of irradiation, Fig.6. PNA-OG-100 mineralizes to 84% by 40 min of microwave irradiation, while PNA-OG-50 mineralizes to 86% by 20 min irradiation. Although, the pure dye solution reveals decolourization/degradation under microwave irradiation, from the beginning of the experiment, further degradation of some of the intermediates into smaller moieties are retarded due to factors related to energetics of the chemical reaction. However, PNA provides the surface for the adsorption of these intermediates and $OH^{\bullet}$ free radicals, and lowers the interaction energies causing further degradation of the intermediates resulting into mineralization. It is expected that microwave exposure of one hour or beyond will mineralise the dye solution to negligible TOC value.

Mechanism of free radical formation

Microwave irradiation has been variously attributed with nonthermal effect to account for the exceptionally fast organic reactions and higher yield[32]. Many scientists have observed that the nonthermal effect associated with microwave irradiation enhances the dye degradation when coupled with UV-VIS radiation in presence of a photocatalyst[33-38]. *Horikoshi et al.*[36-37] have reported that the generation of free hydroxyl radical is significantly enhanced under photocatalytic condition in a microwave oven run at 21°C. It was also observed that when the temperature was increased the free radical formation decreased. Apparently, in our study, the ambient temp of 30°C of the reaction medium also helps in enhancing the nonthermal effect and splitting of H_2O molecules into free radicals. Incase of the degradation of 2,4-D (2,4,dichlorophenoxy acetic acid), *Horikoshi et al.*[35] established that greater efficiency of microwave-assisted processes was due to nonthermal effect of microwave in the breakup of aromatic ring of 2,4-D (oxidation), but not so in the dechlorination process (reduction), for which microwave had only negligible influence. *Horikoshi et al.*[36-37] even attributed 'mysterious effect' to microwave radiation in relation to chemical reactions. In chemical reactions carried under microwave irradiation, therefore, nonthermal effects are quite significant; this holds in our case too. In a solution of dye in water, the water molecules are adsorbed on the dye molecules preferably on the polar sites, like azo and sulphonate groups Water molecules undergo orientation polarization under microwave irradiation, but because of attractive pull of the azo/ sulphonate groups of the dye molecules, they undergo enormous twisting which weakens the H….OH bond. Vibrations of sulphonate/azo groups also stretch out H….OH bond, all these forces in combination may cause splitting of water molecules into free radicals. Hot spot formation and other not well defined nonthermal effects under the conditions of microwave oven used can make the H_2O molecules susceptible to fragmentation into free radicals such as $H^{\bullet}$ and $OH^{\bullet}$. We presume that only under proper physical and chemical conditions, the water molecules split into free radicals by microwave radiations, Scheme.1 .Two of these conditions are the presence of strong polar molecules like dye (OG) and the near ambient temperature in the microwave oven.

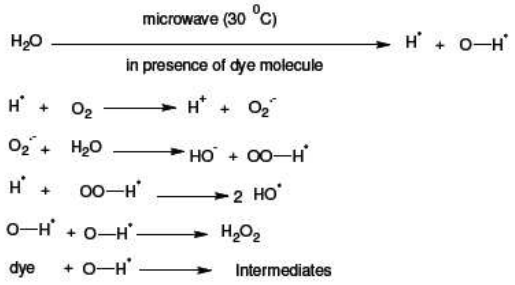

Scheme 1 Free radical formation

As has been found by other authors hydroxyl radical is the main oxy species which initiates and sustains the degradation of the dye[35-38]. The presence of $OH^{\bullet}$ free radicals and its participation in the degradation of the dye molecules can be confirmed by isopropyl alcohol, a scavenger of $OH^{\bullet}$. When isopropyl alcohol (5 mmol/ L) was added in the 100 ml of OG-100 solution and exposed to microwave radiations the degradation was completely stopped as no decrease in the intensity of 480 nm peak was noticed. On adding the scavenger at the rate of 0.1 mmol/L in the same amount of dye solution and exposing to microwave radiation at 30°C, slow decrease in the peak intensity at 480 nm was observed. This shows that dye degrades slowly as $OH^{\bullet}$ was removed slowly, the k value in this case was found to be low, 0.008, Fig.7. Benzoquinone (0.1mmol/L) when added similarly in the dye solutions and exposed to microwave irradiation as mentioned before reveals slow degradation of the dye and the k value was found to be 0.0066, Fig.7 (inset). This shows that $O_2^{\bullet-}$ free radical was also formed during the degradation of the dye. H_2O_2 is generated by recombination of two $OH^{\bullet}$ free radicals. Generation of H_2O_2 was confirmed spectrophotometrically in partially degraded dye solution. H_2O_2 was found to increase as the decolourisation proceeded. The amount of H_2O_2 at 10 and 20 min irradiation time for OG-100 dye solution was found to be less, 4 and 10 µmol/L.

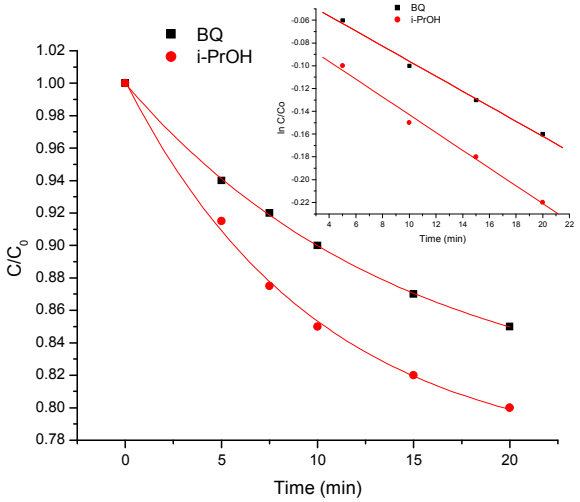

Fig.7 C/Co Values for i-PrOH and BQ (inset shows ln C/Co values)

HPLC results show peaks corresponding to different retention times, Table 2. MS peaks of degraded dye samples at different retention times are shown in Table 2. Except the first intermediate at 100% abundance, two or more intermediates with lower abundance are obtained[38]. The first intermediate with 100% abundance is taken as the main degradation product at the corresponding retention time[38]. It is worth mentioning that in this study, we get intermediates with low m/z values, from 227 to 97. The dye thus degrades considerably. The intermediates are labeled as A1, A2, A3, A4, A5, A6, A7, and the parent dye as P1, as shown in Fig.8 (a). Above m/z 227, no prominent intermediate was found. In one case, an intermediate of m/z 300 was encountered. We have therefore taken A1 as the intermediate from parent dye PI which generates intermediates from m/z 227 - m/z 97. A tentative degradation pathway is proposed in which observed intermediates are produced by attack of $OH^{\bullet}$ free radicals. The intermediates reveal that degradation proceeds via elimination of sulphonate groups, asymmetric/symmetric cleavage of diazo group and its oxidation, and random non

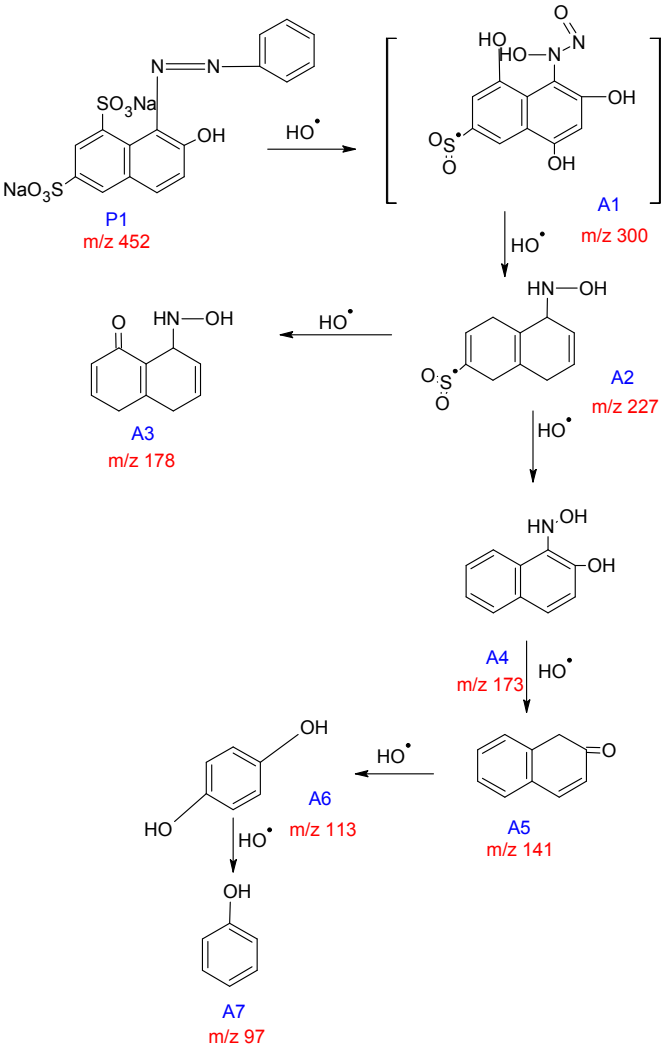

Fig.8 (a) Identification of intermediates

preferential attack on carbons of naphthalene ring resulting in its cleavage and oxidation, all through attack by $OH^{\bullet}$ free radicals[21]. A1 (m/z 300) [(dioxido{ 4,6,8 trihydroxy-5-[hydroxyl (nitroso)amino] naphthalene-2-yl}-sulphanyl))], is obtained from parent dye P1 by elimination of one SO_3Na group at C4, removal of ONa from the SO_3Na at C2, hydroxy formation at C4, C6 and

C8, elimination of aromatic ring at diazo bond at C5, and oxidation of diazo group, all through attack of $OH^{\bullet}$ free radicals. A1 degrades to A2 (m/z 227), by elimination of one nitroso group and formation of NHOH at C5, elimination of the 3 hydroxyl groups from C4, C6, and C8, all through reaction with $OH^{\bullet}$, resulting into [{5-(hydroxyamino)-1,4,5,8 tetrahydro naphthalene-2-yl} (dioxido)- sulphanyl]. A2 degrades to A3 (m/z 178) [8-(hydroxyamino)-4,5,8 trishydro naphthalene-1-one], by elimination of SO_2 group from C2 and oxidation at C4 of A2 by reaction with $OH^{\bullet}$ free radicals. A2 degrades by another route to A4 (m/z 173) [1-(hydroxyamino)-naphthalene-2-ol], by elimination of SO_2 group at C2 and formation of hydroxyl group at C6 of A2 through reaction with $OH^{\bullet}$ free radicals. A3 can also form A4 through conversion of quino group into hydroxyl group by reaction of $OH^{\bullet}$ free radicals at C1 of A3, and mechanistic

Table 2 Intermediates found at different retention times

Retention time	Intermediates with % abundance
OG-100	
3.95 min	97(100%), 201(85%), 120(28.57%)
4.27 min	141(100%), 95(15.78%), 195(25%)
5.39 min	178(100%), 89(63.8%), 241(56.9%)
6.59 min	227(100%), 59(93%), 113(57%), 300(21.4%)
12.22 min	113(100%),227(40.75%), 300(6.25%)
12.29 min	173(100%),178(40%), 89(26.6%)
PNA-OG-100	
4.0	200.97 (100%), 97 (37%)
4.31	209.85 (100%), 140.98 (80.7%), 62.02 (40.85%)
4.57	226.9 (100%), 120.98(69.4%), 113 (32.5%)
5.30	113(100%), 120 (69.4%), 240.98 (76.2%)
6.58	222 (100%), 207(35.7)
11.74	113 (100%), 227(68.2), 300 (68.2%), 59.9 (29.4%)
12.25	113 (100%), 227(18.8%)

rearrangement to locate hydroxyl group at C7. A4 degrades into A5 (m/z 141) [naphthalene-2(1H)-one] by elimination of hydroxylamine group at C1 and oxidation at C2 of A5 by attack of $OH^{\bullet}$ free radicals. A5 changes to A6 (m/z 113) [benzene-1,4-diol], by elimination of one aromatic ring and addition of two hydroxyl groups at C2 and C5 of benzene ring through reactions of $OH^{\bullet}$ free radicals. Elimination of one hydroxyl group from A6 at C2 through reaction with $OH^{\bullet}$ free radicals results into A7, (m/z 97) [phenol]. Mass spectra also shows the presence of acetic acid (m/z 59), Table 2. These observations lead to the conclusion that in the present experimental setup, microwave irradiation degrades the dye into intermediates with low molar masses like phenol and acetic acid ultimately leading to mineralization.

LC-MS analysis of the dye solution in presence of PNA reveals the intermediates at various retention times, Table 2**.** The above table shows that in presence of PNA, PNA- OG -100 dye solution degraded into intermediates of m/z: 227, 222, 210, and 113. The intermediate m/z: 113 was the main product at retention times 5.30 min, 11.74 min and 12.25 min, and intermediate m/z: 210 at retention times 4.0 min and 4.31 min. It is therefore clear that parent dye degrades fast into intermediates of smaller molar mass. Intermediates with molar mass less than m/z 113, like m/z 97, 62, and 59.9, were also encountered. This shows that degradation in presence of PNA was fast and continued to form intermediates of smaller molar masses which were not recorded by the MS system.

The intermediates of m/z 222 [4,8 dihydroxy-1-(nitrosoamino) naphthalene-2 (1H)-one] and 210 [8-(dihydroxyamino)-7-8-dihydronaphthalene-1,7-diol] have molecular structures related to m/z 227 and thus make the part of the degradation pathway. These intermediates are shown in Fig.8 (b).

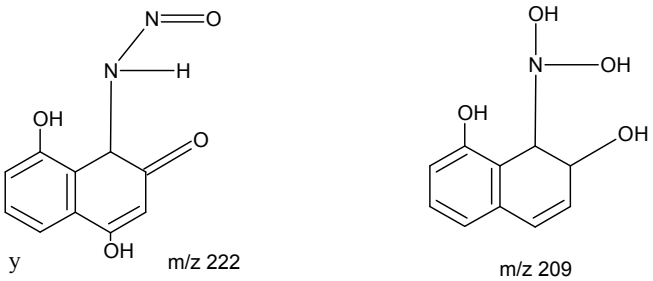

Fig.8 (b) Identification of alternate intermediates

Toxicity studies

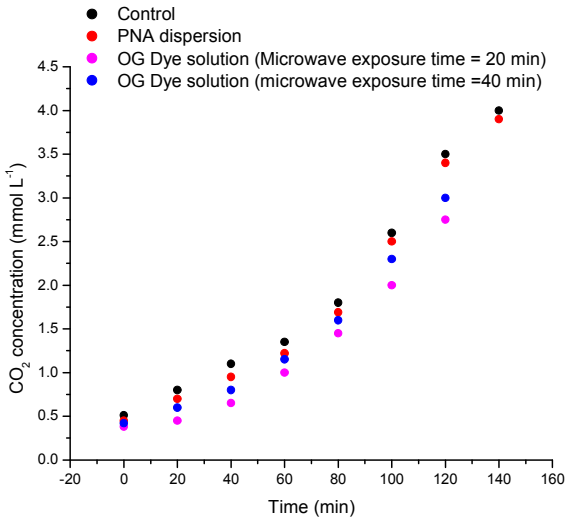

Fig.9 CO_2 evolution in control and test solutions at different incubation times.

The acute toxicity was evaluated by monitoring the respiration inhibition in *Escherichia coli* cultures submitted to the contaminants. Acute toxicity of the dye solutions exposed to microwave irradiation for 20 min and 40 min in terms of % inhibition of bacterial growth against the control bacterial culture was detemined from the Fig.9. Since the original dye solution degraded into mixture of fragments of low molar masses, we thought to determine the acute toxicity levels of these degraded

products. It is noticed that for 20 min and 40 min microwave irradiation, acute toxicity (% inhibition) of OG-PNA dye solution was 25% and 16 %. The PNA dispresion showed CO_2 evolution matching with the control. As was observed earlier if microwave exposure is further enhanced, the acute toxicity level is expected to further go down.

Conclusion

Microwave irradiation was found to decolorize OG dye solution even in absence of UV-visible radiation and inorganic photocatalyst in the microwave oven used at 30°C. PNA, was found to enhance the rate of degradation. In presence of PNA, 100 ml of 100 ppm dye solution degraded to 90% in 20 min, while the same solution of dye in absence of PNA degraded only to 45% in the same time. PNA was found to enhance the mineralization of the dye substantially. 100 ppm OG dye solution with PNA was mineralized to 84% in 40 min, while the same dye solution without PNA showed only 45% mineralization in the same period. The mineralization occurred through adsorption of intermediates on PNA-catalyst surface and their further degradation by reaction with $OH^{\bullet}$ free radicals. The degradation was attributed to the generation of $OH^{\cdot}$ free radicals by nonthermal effects of microwave irradiation. At PNA surface the naphthalene ring and sulphonate groups undergo chemical modification much faster than modification or elimination of azo groups. The dye degrades in aqueous solution through pseudo first order rate kinetics. LC-MS results also establish the degradation of the Orange G dye into intermediates of smaller molar masses. Molecular structure was assigned to intermediates of varying m/z values and a tentative degradation pathway was proposed. The above analysis also shows that PNA or its fragments do not pass into dye solution/water as no fragments related to the former are detected by LC-MS. PNA is thus safe to use as catalyst in the degradation of the dye under microwave irradiation.

Acknowledgement

The corresponding author Dr.Ufana Riaz also wishes to acknowledge the University Grants Commission, India for granting major research project vide sanction no. F.NO. 41-199/2012(SR).

References

1. C.Rafols, D.Barcelo, *J.Chromatogr. A*, 1997, **777**,177-181.
2. H.Houas, H.Lachheb, M.Ksibi, E.Elaloui, C. Guillard, J-M. Hermann, *Appl. Catal.B: Environ*., 2001, **31**, 145-157.
3. U.Pagga, D.Brown, *Chemosphere*, 1986,**15**,479-491.
4. M. Boeninger in *Carcinogenicity and Metabolism of Azo Dyes Especially those Derived from Benzidine*, DHHS (NIOSH) Publication, Government Printing Office, Washington, DC, 1990, pp. 80-119, US.
5. F.Rafii, W. Franklin, C.E. Cerniglia, *Appl.Environ.Microbiol*., 1990, **56**, 2146-2151.
6. S.Yang, P.Wang, X.Yang, G.Wei, W.Zhang, G.L. Shan, *J.Hazard.Mater*., 2010,**179(1-3)**, 552-558.
7. S.Horikoshi, A.Saitou, H.Hidaka, N.Serpone, *Environ.Sci.Technol.,* 2003, **37(24)**, 5813-5822.
8. H.Wang, J.Niu, X.Long, Y.He, *Ultrason.Sonochem*., 2008, **15(4)**, 386-392.
9. IARC (International Agency for Research on Cancer) (2010). IARC Monographs on the Evaluation of Carcinogenic Risks to Humans. V. 93. Carbon Black, Titanium Dioxide, and Talc. Retrieved December 12, 2010, from http://monographs .iarc.fr/ENG/Monographs/vol93/mono93-7.pdf
10. N.S.Wigginton, K.L.F.Haus, M.Hochella, *J. Environ.Monitor.,*.2007, **9**, 1306-1316.
11. R.Kaegi, A.Ulrich, B.Sinnet, R.Vonbank, A.Wichser, S. Zuleeg, H.Simmler, S.Brunner, H.Vonmont, M.Burkhardt, M.Boller, *Environ.Poll*., 2008, **156**,233-239.
12. S.Min, F.Wang, Y.Han, *J.Mater.Sci.* 2007,42,9966-9972.
13. B.Wang, C.Li, J.Pang, X.Qing, J.Zhai, Q.Li, *Appl.Surf.Sci*., 2012, **258(1)**, 9989-9996.
14. V.Církva, H.Žabova, M.Hájek, *J.Photochem. Photobiol.A*, 2008, **198(1)**, 13-17.
15. X.Zhang, D.D.Sun, G.Li, Y.Wang, *J.Photochem.Photobiol.A* 2008, **199(2-3)**, 311-315.
16. S.Horikoshi, H.Hidaka, N.Serpone, *J.Photochem.Photobiol. A*, 2004, 161(2-3), 221–225.
17. S.Horikoshi, H.Hidaka, N.Serpone,*Chem.Phy.Lett*., 2003, **376(3-4)**, 475-480.
18. D.P. Wang, H.C. Zeng, *Chem.Mater*. 2009, **21**, 4811-4823.
19. U.Riaz , S.M. Ashraf, *Sep.Purif.Technol*., 2012, **95(12)**, 97-102.
20. U.Riaz,S.M. Ashraf, *Chem.Engg. J.,* 2011, **174(2-3)**, 546-555.
21. J.R.Guimarães, C.R.T. Farah, and P.S. Fadini, *J. Braz. Chem. Soc*,.2012, **23**, 461-467.
22. M.Stylidi, D.I. Kondarides, X.E. Verykios, *Appl.Catal.B: Environ.,* 2004, **47(3)**, 189-201.
23. U.Riaz, S. Ahmad and S.M. Ashraf, *Des.Mono.Polym*., 2008, **11(2)**, 201-214.
24. Y.Cao, P.Smith, A.J. Heeger, *Synth.Met.,* 1992, **48(1)**, 91-97.
25. C.H.Lim, Y.J.Yoo,*Proc.Biochem*., 2000, **36(3)**, 233-241.
26. B.K.Kim, Y.W.Kim, K.Won, H.Chang, Y.Choi, K.J. Kong, *Nanotechnol.,* 2005, **16**, 1177-1181.
27. R.Cruz-Silva, J.Romero-Garcıa, J.L.Angulo-Sanchez, A. Ledezma-Perez, E.Arias-Marı´n, I.Moggio,E.Flores-Loyola, *Eur.Polym.J.,* 2005, **41**, 1129–1135.
28. S-C.Kim, P.Huh, J.Kumar, B.Kim, J-O. Lee, F.F. Bruno and L.A. Samuelson, *Green Chem*., 2007,**9**, 44-48.
29. H.Chenini, K.Djebbar, S.M.Zendaoui, T.Sehili, B.Zouchoune, *Jord. J.Chem.*, 2011, **6(3)**, 307-319.
30. X-R.Xu, X-Z. Li, *Sep.Purif.Technol*. 2010, **72**, 105-111.
31. M.A. Meetani, M.A.Rauf, S.Hisaindee, A.Khaleel, A. AlZamly, A. Ahmad*, RSC Adv*., 2011, **1**, 490-497.
32. C.O.Kappe, D.Dollinger, *Chem.Rev.,* 2001, **107**, 2563-2591.
33. J.H.Booske, R.F.Cooper, I. Dobson, *J.Mater.Res.,* 1992, **77(2)**, 495-501.
34. S.Horikoshi, A.Tsuchida, H.Sakai, M.Abe, S.Sato, N.Serpone, *J.Photochem.Photobiol.A*, 2009, **8**, 1618-1625.
35. S.Horikoshi, H.Hidaka, N. Serpone, *J.Photochem.Photobiol.A,* 2003, **159(3)**, 289-300.
36. S.Horikoshi, N.Serpone*, J.Photochem. Photobiol.C Photochem.Rev*., 2009, **10**, 96-110.
37. S.Horikoshi, F.Sakai, M.Kajitani, M.Abe, A.V.Emeline, N.Serpone, *J.Phy.Chem.C*, 2009, **113(14)**, 5649-5657.
38. C.E.Clarke, F.Kielar, H.M.Talbot, K.L. Johnson, *Environ.Sci.Technol*., 2010, **44**, 1116-1112.

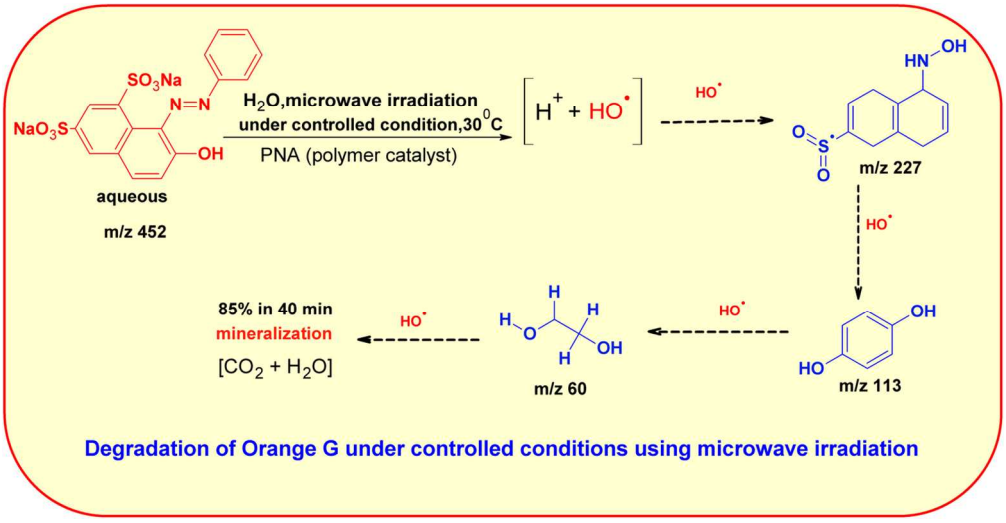

126x64mm (300 x 300 DPI)